Earth Syst. Dynam. Discuss., 6, 907–941, 2015
www.earth-syst-dynam-discuss.net/6/907/2015/
doi:10.5194/esdd-6-907-2015

Earth System Dynamics
Discussions
Open Access

Climatology of Vb-cyclones, physical mechanisms and their impact on extreme precipitation over Central Europe

M. Messmer[1,2], **J. J. Gómez-Navarro**[1,2], **and C. C. Raible**[1,2]

[1]Climate and Environmental Physics, Physics Institute, University of Bern, Bern, Switzerland
[2]Oeschger Centre for Climate Change Research, University of Bern, Bern, Switzerland

Received: 18 March 2015 – Accepted: 8 April 2015 – Published: 4 May 2015

Correspondence to: M. Messmer (messmer@climate.unibe.ch)

Published by Copernicus Publications on behalf of the European Geosciences Union.

Abstract

Cyclones, which develop over the western Mediterranean and move northeastward are a major source of extreme weather and known to be responsible for heavy precipitation over Central Europe and the Alps. As the relevant processes triggering these so-called Vb-events and their impact on extreme precipitation are not yet fully understood, this study focusses on gaining insight into the dynamics of past events. For this, a cyclone detection and tracking tool is applied to the ERA-Interim reanalysis (1979–2013) to identify prominent Vb-situations. Precipitation in the ERA-Interim and the E-OBS datasets is used to evaluate case-to-case precipitation amounts and to assess consistency between the two datasets. Both datasets exhibit high variability in precipitation amounts among different Vb-events. While only 23 % of all Vb-events are associated with extreme precipitation, around 15 % of all extreme precipitation days (99 percentile) over the Alpine region are induced by Vb-events, although Vb-cyclones are rare events (2.3 per year). To obtain a better understanding of the variability within Vb-events, the analysis of the 10 heaviest and lowest precipitation Vb-events reveals noticeable differences in the state of the atmosphere. These differences are most pronounced in the geopotential height and potential vorticity field, indicating a much stronger cyclone for heavy precipitation events. The related differences in wind direction are responsible for the moisture transport around the Alps and the orographical lifting along the Alps. These effects are the main reasons for a disastrous outcome of Vb-events, and consequently are absent in the Vb-events associated with low precipitation. Hence, our results point out that heavy precipitation related to Vb-events is mainly related to large-scale dynamics rather than to thermodynamic processes.

1 Introduction

High impact weather events may have dramatic impacts on society, being a problem that could be potentially enhanced under a changing climate (IPCC-SREX, 2012). Such

ESDD
6, 907–941, 2015

events lead not only to great economical, but also to personal damage (Donat et al., 2011). Tropical but also extratropical cyclones can certainly be classified as high impact weather events, as they are associated with extremely strong winds and heavy precipitation that eventually can lead to floodings (Fink et al., 2012; Raible, 2007; Stucki et al., 2014). In Central Europe, and more precisely in the Alpine region, a source of high impact events is the so-called Vb-cyclone. Such type of cyclone was first mentioned by Köppen (1881), and later defined by Van Bebber (1891) in a cyclone classification based on its characteristic pathway (Fig. 1). The categories were labelled according to Roman numeration from one to five. The Vb-track (a subcategory within the fifth category, and the only one still in use) is associated with extreme precipitation and flash floods over Germany, Austria, Switzerland, the Czech Republic and Poland. The origin of Vb-cyclones are either the Bay of Biscay, the Balearic Sea or the Ligurian Sea, where moisture uptake occurs. The cyclone moves eastward via Italy and the Adriatic Sea, before it turns northward to the Black Sea or Saint Petersburg. Along this track, orographically induced rainfall takes place on the northern side of the Alps. Hereinafter the expression "Vb-cyclone" is used for cyclones that follow van Bebber's track.

Despite the destructive potential of Vb-cyclones, literature provides only little information about its characterisation. Most studies on Vb-cyclones focus on case studies. For instance the one-in-a-century flood in August 2002, induced by a Vb-cyclone, has been analysed extensively (Ulbrich et al., 2003a, b; Grazzini and van der Grijn, 2002; Stohl and James, 2004; James et al., 2004; Kaspar and Müller, 2008). A main focus in these studies is the moisture source. Although the Mediterranean Sea is an important source for precipitable water, other studies suggested that the evaporation from land contributes to the precipitation amounts (Ulbrich et al., 2003a; Stohl and James, 2004; Sodemann et al., 2009). Additionally, the Atlantic Ocean and long-range advection of moisture cannot be despised, as demonstrated by Sodemann et al. (2009) using a tracer for water vapor. Another focal point is set on the synoptic-scale conditions leading to the extreme event in August 2002 (Ulbrich et al., 2003b; Grazzini and van der Grijn, 2002). Ulbrich et al. (2003b) suggested a positive interference of several factors

ESDD
6, 907–941, 2015

that occured in August 2002. These factors include advection of humidity, a quasi-stationary tropospheric trough, inducing upper-level divergence, and orographic lifting of the surface low. Grazzini and van der Grijn (2002) concluded that the anomalous large-scale situation in the summer 2002 and the associated increased cyclone-activity is the main reason for the devastating floods in August 2002. Other Vb-cyclones that appear as case studies in literature are the cyclone "Axel", in July 2001, which is related to the Vistula flood (Kundzewicz et al., 2005). More important for Switzerland is the Vb-cyclone in August 2005, which led to a very severe flood on the northern flanks of the Alps (Beniston, 2006). The author found that the peak rainfall occurs in August, and is due to a combination of warm ground surfaces and moisture convergence into the Alpine region.

Fewer studies go beyond case studies and analyse a Vb-cyclone climatology. Hofstätter and Chimani (2012) provided an objective catalogue of Vb-cyclones, which allowed the authors to infer that these are only rare events (3.5 year^{-1}) with a peak occurrence during April. Nissen et al. (2013) focused on the summer half year of a future climate. They projected a decrease in the total number of Vb-cyclones, although their related mean precipitation increases. An extended study, considering the last 500 years of flood history, only found a weak relation between Vb pathways and flood occurrence (Mudelsee et al., 2004). Although there is only little literature specifically focused on climatological Vb-cyclone characteristics, there are several studies devoted to the cyclones in the Mediterranean region, a more general category to which the Vb-cyclones belong to. Trigo et al. (1999) performed an objective climatology of cyclones in the Mediterranean region, concluding that the Genoa region, which is also the origin of Vb-cyclones, generates most of the cyclones in the Mediterranean region. The authors also stated that topography-controlled cyclogenesis regions account for the most intense events. Fricke and Kaminski (2002) showed that the period from 1881 to 2001, which includes the most extreme precipitation events, reveals a more frequent appearance of the weather pattern "trough over Middle Europe" (Fricke and Kaminski, 2002).

ESDD
6, 907–941, 2015

This pattern encloses also the Vb-cyclones. Hence, Vb-cyclones show all the prerequisites needed to trigger high-impact weather events.

Cyclones in the Mediterranean region are frequently analysed under future climate change, as the Mediterranean Basin is a key hotspot of societal vulnerability (IPCC-AR4, 2007). Unfortunately, there is still no clear agreement on the trend in cyclone number in a future climate. Some studies concluded that there will be a general decrease in number of cyclones during the entire year (Lionello et al., 2002; Nissen et al., 2014) or just in winter (Pinto et al., 2006; Raible et al., 2010), due to either a polar shift of cyclones, a positive shift of the NAO, changes in baroclinicity or static stability. However, other analyses reported an increase in the total number of cyclones over the Mediterranean (Muskulus and Jacob, 2005; Nissen et al., 2014). The studies also disagreed with respect to extreme events, where Lionello et al. (2002) and Pinto et al. (2006) found an increase, whereas Muskulus and Jacob (2005) and Nissen et al. (2014) found a decrease of extreme cyclones in the Mediterranean. Additionally, Muskulus and Jacob (2005) indicated no significant changes concerning the track properties and precipitation. This is in contrast to Gao et al. (2006), who found a pronounced decrease, especially in summer precipitation, due to an intensified anticyclonic ridge. Nonetheless an increase in precipitation events, especially over and around the Alpine region, can be expected especially in winter according to the study of Gao et al. (2006) due to the fine scale structures in the Alps. The lack of consistency that emerges from these studies illustrates the difficulties involved in climate projections, and point out that a deeper process understanding is important to reduce uncertainties.

As outlined above, only basic climatologies of Vb-cyclones in the past (Hofstätter and Chimani, 2012) and the future (Nissen et al., 2013) have been performed so far. However, a comprehensive analysis concerning the triggering mechanisms driving the extreme precipitation associated with Vb-cyclones is still missing. Thus, in this study we provide a climatology of Vb-cyclones and also explore the physical mechanisms that impact precipitation amounts of Vb-cyclones. The climatology is performed for

ESDD
6, 907–941, 2015

a 35 yr period using the ERA-Interim reanalysis, whereas the physical mechanisms are studied in more detail for Vb-cyclone subcategories.

The structure of this paper is as follows: Sect. 2 provides an overview of the datasets and methods used in the study. Section 3 describes the basic climatology of Vb-cyclones, gives insight into the Vb-cyclone variability, and investigates their underlying physical mechanisms. Finally, Sect. 4 provides a summary and discussion of the results, presenting also a short outlook.

2 Data and Methods

2.1 Reanalysis and observational datasets

This study is based on ERA-Interim, a global atmospheric reanalysis data set (Dee et al., 2011) produced by the European Centre for Medium-Range Weather Forecasts (ECMWF). ERA-Interim provides 6 hourly estimates of three-dimensional meteorological parameters and 3 hourly estimates for surface variables for the time period between 1979 to present. The ERA-Interim dataset is generated by running the 2006 version of the Integrated Forecast System model of the ECMWF with a resolution of T255 (approximately 80 km) and 60 vertical levels up to 0.1 Pa. The system assimilates observational data with a 4-dimensional variational analysis (4-D-Var) in a 12 h analysis window. A number of observational datasets are assimilated in the final product ranging from satellite data to surface pressure observations and radiosonde profiles (see Sect. 4 in Dee et al., 2011).

In this study we analyse Vb-cyclones for the 35 year period 1979–2013 at 6 hourly resolution. To facilitate the comparison, the 3 hourly forecasted precipitation data is accumulated to 6 hourly data. Furthermore, a vertical integration of moisture in the atmosphere is computed to obtain the total amount of precipitable water. As precipitation data in ERA-Interim is predicted using a forecast model, they are subject to spin-up and spin-down effects that need to be kept in mind (Dee et al., 2011).

ESDD
6, 907–941, 2015

Since some important results in this study are based on precipitation amounts, and given that ERA-Interim reanalysis suffers from the aforementioned spin-up and spin-down effects, the precipitation data are compared to the purely observational gridded product E-OBS (Haylock et al., 2008). The E-OBS data are based on weather station data and are interpolated to a 25 km grid. It is a European land-only, daily, gridded dataset. Several variables are available: precipitation, sea level pressure and mean, minimum and maximum temperature for the period 1950 to 2013 (Haylock et al., 2008). As this dataset is based on observations only, there are a number of limitations that need to be mentioned. On the one hand the observations show several inhomogeneities in space and time that populate observational products with uncertainties rendering them mutually inconstant even in areas properly covered by observations (Gómez-Navarro et al., 2012). The spacial inhomogeneity is due to a different density of the observational network of each country, whereas the temporal heterogeneity is based on the varying number of stations maintained by the countries (Hofstra et al., 2009). On the other hand precipitation is especially afffected by uncertainties over mountain areas, such as the Alps, our region of interest. Note that the uncertainties are maximal in the summer, as precipitation is driven by convection (Hofstra et al., 2009). This form of precipitation is very local, and thus difficult to capture with the sparse network covering the Alps (Hofstra et al., 2009).

2.2 Detection and tracking methods

In this study we use a tool developed by Blender et al. (1997) that automatically detects and tracks all types of cyclones within a certain area. Thus, in a first step all cyclones that occur over Western and Central Europe during the 35 year time period are retained. Note that there is an overall agreement in climatological characteristics of midlatitude cyclones between different tracking and detection methods (Raible et al., 2008; Neu et al., 2013).

The technique has a number of free parameters that allow to adjust the search according to specific purposes. In our case, these parameters are fit to special character-

ESDD
6, 907–941, 2015

istics of Mediterranean cyclones. In particular, since they develop as shallow low-level cyclones, weak gradients must be chosen in order to be able to detect these at the beginning of their life cycle. The position of the cyclones is identified by local minima in the geopotential height at 850 hPa (z850), taking the eight neighbouring grid points into account. The minimum gradient around a cyclone centre in an area of $1000 \times 1000\,km^2$ is used to focus on cyclones, thus filtering out polar and weak minima such as heat lows. For this study we applied a minimum gradient of 25 m/1000 km. Additionally, a maximum gradient of 50 m/1000 km must be reached at least once during the life cycle of a cyclone. The minimum lifetime of each cyclone is set to 24 h. The minima are combined by a next neighbourhood search within a distance of 1000 km. This threshold is chosen as it resembles roughly the Rossby deformation radius.

Since the Alps introduces disturbances into the geopotential height field, and to remove small-scale and secondary low pressure centres, the input data z850 from ERA-Interim is previously low-pass filtered using a weighted average of 5×5 grid points prior to the analysis of the tracks. The weights are defined according to a Hann-window function. The 5×5 window has been chosen by analysing the robustness of the obtained trajectories after different window sizes are applied in the smoothing (not shown). Similarly, several levels of the geopotential height fields are tested within the detection and tracking technique, using finally the 850 hPa level. The reason is on the one hand to have a balance between the shallow character of Mediterranean cyclones and therefore a level close to the ground. On the other hand, it is hardly possible to find meaningful tracks at the surface, as mountains introduce substantial artefacts into the geopotential height field that render the cyclone tracking more difficult. Tests with several levels and filters have shown that the prominent Vb-cyclones (Alpine flood 2005, Elbe flood 2002, Axel 2001) can be identified in the 850 hPa level in combination with a 5×5 grid point weighted average low-pass filter, so this is the configuration employed through the manuscript.

As the tracking tool detects all cyclones, not only Vb-cyclones, the output of this tool has to be further filtered. For this task, we define areas (boxes) where a potential Vb-cyclone should pass (or not to do it) at least once in its lifetime in order to be retained: the origin box (42–46° N, 4–13° E) accounts for the fact that Vb-cyclones, per definition, either develop or intensify over the Mediterranean Sea close to Genoa, while the end box (46–52° N, 12–19° E) assures the sudden turnaround northward at the eastern edge of the Alps. A third restrictive box (46.5–55° N, 5–11.5° E) covering the Alps and the eastern part of Germany is introduced to avoid that cyclones that directly cross the Alps are classified as Vb-cyclone. These three boxes are displayed in Fig. 2 and are labeled with O for the origin, E for the end and R for the restriction box. Note that this simple criterion is similar to that described by Hofstätter and Chimani (2012).

2.3 Composite analysis of midlatitude cyclones

A prominent problem when analysing the structure and physical processes related to cyclones is that they do not occur at a fix location, but they are moving objects. Hence, a simple temporal mean becomes misleading due to the different location of the storm. A simple approach to overcome this problem is to use a moving grid whose centre coincides with the storm at each time step. However, this still has a problem when the analysis is performed on a regular latitude–longitude grid (as is the case of ERA-Interim). This is so because the area of each grid box relative to the centre of the cyclone decreases with higher latitudes, so each grid point might be representative of a different area in different time steps if the storm moves northward. This is not a major problem in tropical cyclones, since the effect becomes insignificant near the equator, but it is a matter of concern in the midlatitudes, precisely where Vb cyclones evolve. Since this study aims at analysing temporal composites of several variables, or the most precipitation intense time step in different cyclones, this becomes a technical challenge that has to be addressed.

This study applies a composite tool based on the projection described by Bengtsson et al. (2007). The method works as follows. The variable of interest, defined on a latitude–longitude grid, is first remapped onto spherical coordinates in a $0.5^\circ \times 0.5^\circ$ resolution grid, where the cyclone's centre is set in the pole of the grid. Hereby, a spherical cap around the storm is obtained for each time step. This cap has an outermost boundary located at 23° off the cyclone centre. Once the variable of interest is remapped onto this grid (which is different for each time step), all regular statistics can be calculated over this variable (means, maximum, etc.), and the results are fully comparable among different time steps and storms.

3 Results

3.1 Basic climatology of Vb-cyclones

Vb-cyclones are relatively rare events compared to the frequency of cyclones detected over Europe. Applying the tracking approach of Blender et al. (1997) to the smoothed z850 surface, 3448 cyclones are detected over Europe between 1979 and 2013. After filtering out the cyclones with the boxes described in Sect. 2, a total of only 82 cyclones is classified as Vb-cyclones, i.e., only 2.4 % of all cyclones in Western and Central Europe. Due to their rareness, the average appearance of Vb-cyclones per year is 2.3, with a mean duration of 3.1 days. Still, the occurrence of these events is irregularly distributed over the 35 year period (for instance up to five Vb-cyclones are tracked in 1979 and 1984, while none is found in the years 1989, 1993 and 2011). However, despite their rareness they are responsible for almost 15 % (14 %) of extreme precipitation days in the Alpine region considering ERA-Interim (E-OBS) dataset in this period of time. Here, extreme precipitation days are defined as exceedances of the 99 percentile. Hence, we note that even though Vb-events are relatively rare, they have a great potential to trigger high-impact weather events.

Using a similar approach, Hofstätter and Chimani (2012) reported an annual average of 3.5 Vb-cyclones per year. The climatological probability of Vb-cyclones to appear on any day is 3.8 % in their analysis, compared to the 2.0 % found in the present study. The potential reason for this discrepancy is that their method substantially differs from the one used here: different input data, tracking tool, and posterior filtering. Still, 62 %

ESDD
6, 907–941, 2015

of the Vb-cyclones tracked in this study coincide with those found by Hofstätter and Chimani (2012) considering only the overlapping period from 1979 to 2002 of the two studies.

Beyond the irregular distribution of the 82 Vb-cyclones over the analysed period, they are also not evenly distributed within the annual cycle. Considering the standard seasons winter (December, January, February), spring (March, April, May), summer (June, July, August) and autumn (September, October, November) there are less Vb-cyclones in winter than expected from a homogeneous distribution over the annual cycle (p level < 0.1) and an excess in spring (p level < 0.05). The fact that Vb-cyclones emerge more frequently in spring has already been pointed out by Van Bebber (1891) and confirmed by Hofstätter and Chimani (2012), which reported a maximum in April.

The Vb-cyclones are also characterised by their trajectories. The probability density of all Vb-cyclone centers is depicted in Fig. 3 and estimated using a Gaussian Kernel Density Estimator with a bandwidth of 0.6°. Thus, the shaded area indicates how likely it is that a Vb-cyclone center passes through this grid point at any time step. The density illustrates the most common pathways followed by Vb-cyclones, and fits very well the track described by Van Bebber (1891), illustrating why this categorisation is still in use. As expected the Genoa region is most frequently passed by the cyclones, as this region coincides with the origin box. Even a rare Vb-cyclone, which develops in the lee of the Atlas mountain, is detected once. Note that the end of the Vb-cyclone track is more diverse, given that the mature state of the Vb-cyclones is not bound to any box. The effect of the restriction box is clearly visible as sharp bend of the orange-coloured contours at the western flanks of the Alps.

3.2 Within Vb-cyclone variability

In this section we deepen in the analysis of Vb-cyclone characteristics focusing on remarkable differences within these events in particular with respect to precipitation. Thereby, Vb-events are classified by using a precipitation criterion. For this, the mean precipitation over a box covering the Alpine region is calculated for each time step. The

ESDD
6, 907–941, 2015

M. Messmer et al.

box is depicted in Fig. 2 as a black rectangle. As the detected Vb-cyclones may start and end at locations where they are far off a point to exert influence on the aforementioned precipitation area, the composite tool described in Sect. 2.3 is applied to the precipitation field. This step allows to reduce the influence of other weather features on precipitation amounts on the northern side of the Alps. For this analysis, the radius of the cyclone area in the composite tool is adapted from 23° to a more flexible one that depends on the gradient of the cyclone, and thus on its intensity. Hence, Vb-cyclones ascribing a gradient within plus or minus one standard deviation obtain a radius of 6°. Gradients that exceed (fall behind) one standard deviation, 75 (25) percentile or 95 (5) percentile obtain a radius expansion (decrease) of 0.5, 1 or 1.5°, respectively. Only if this radius is able to reach the precipitation box depicted in Fig. 2, the time step is considered as precipitation contributing. In the following, the precipitation of these time steps is accumulated over each Vb-event. Note that this has the disadvantage that the accumulation period differs among various Vb-cyclones, which has to be taken into account in the analysis hereafter.

To compare the precipitation triggered by Vb-cyclones to regular precipitation days, the distribution of such precipitation needs to be estimated. As the Vb-cyclone duration differs from one another, the estimation of the precipitation distribution becomes challenging. Hence, a bootstrap method is applied to estimate such precipitation distribution over this particular box, that has to mimic the real distribution of Vb-cyclone duration. The estimation is based on 3 million bootstrap samples of observed precipitation accumulated during a period whose length is selected randomly according to the observed distribution of length of Vb-cyclones. The same method is applied to the ERA-Interim and daily E-OBS dataset to confirm consistency between observational data and forecasted reanalysis data. Figure 4 displays the estimated distribution of precipitation in the box covering the Alpine region for ERA-Interim. In winter only two (none) of the Vb-cyclones exceed the 95 percentile using ERA-Interim (E-OBS, not shown) dataset, while in summer 24 (19) Vb-cyclones produce extreme precipitation over the region of interest considering ERA-Interim data (E-OBS, not shown). Note

ESDD
6, 907–941, 2015

that there is a wide variability in accumulated summer precipitation within Vb-cyclones, ranging between almost no precipitation and extreme events. Furthermore, most of the winter events show a narrow variability. For consistency reasons and the sake of brevity only the results for ERA-Interim data are shown hereafter, although it has to be noted that the results for the E-OBS dataset resemble the findings based on ERA-Interim discussed here in more detail. The striking difference between summer and winter is most probably due to the effect of the Clausius–Claperyon equation, which relates air temperature to its ability to carry water vapour.

To gain further insight in the characteristics of Vb-cyclones, those related to heavy precipitation events (HPE) and weak precipitation events (WPE) in the extended summer season are analysed in detail. Thereby, the 10 most extreme events with respect to precipitation are selected. Figure 5 displays a composite of the most intense precipitation time step of the 10 HPE on the left and WPE on the right. As expected, the HPEs generate much more precipitation and affect a wider area. Locally, the precipitation amounts are even doubled compared to the WPEs. More interesting is the fact that the HPEs composite shows a precipitation pattern that is expected from Vb-events. The main precipitation falls on the northern flanks of the Alps and extends towards the east as far as the catchment of the river Elbe and Oder, which were the main contributors of the floods in August 2002 (Ulbrich et al., 2003a; Kundzewicz et al., 2005) and thus play an important role in Vb-events. In contrary the WPEs show maximum precipitation more to the east of the Alps. Additionally, there seems to be frontal behaviour that interferes with Vb-cyclones in some of the WPEs which is illustrated by the long precipitation band in Eastern Europe. It is important to note that even though precipitation patterns are different, the associated PDFs of the trajectories of HPEs and WPEs, depicted in the lower panels of Fig. 3, do not show significant differences. Thus, the trajectory of the Vb-cyclone does not seem to play an important role on deciding whether an event will cluster into the HPE or the WPE subcategories.

ESDD
6, 907–941, 2015

3.3 Physical mechanisms driving Vb-cyclones variability

As precipitation amounts are linked to available moisture content in the atmosphere, it makes sense to investigate whether the state of the atmosphere plays a prominent role on the rainfall associated to a Vb-cyclone (Stohl and James, 2004; Sodemann et al., 2009). The precipitable water at the most precipitation intense time step shows a much higher amount for the HPEs, than for WPEs (Fig. 6). Still, the differences around the centre of the cyclone are small compared to the high moisture band further off the centre. The moisture fluxes depicted in Fig. 6 imply that the major part of this moisture is transported straight to the northeast, and thus away from the region of interest for the WPEs and the HPEs. Furthermore, the case-to-case variability is relatively large, and indeed some HPE cases contain even less precipitable water than certain WPEs. Hence, precipitable water in the atmosphere is not an unambiguous variable suitable to predict whether a Vb-cyclone would potentially lead to severe precipitation.

A related variable that is in principle more accurate to characterise the differences observed between HPEs and WPEs is the moisture flux through certain latitude sections of interest. This allows to test the hypothesis generally assumed stating that Vb-cyclones receive most of their precipitable water from the Mediterranean Sea. Therefore, a latitudinal section over the Adriatic Sea is selected as depicted in Fig. 2 with a stippled black line labelled "MED". Results of the moisture flux through this section indicate however that no clear separation of the moisture flux across this line between the HPEs and WPEs is possible (left panel of Fig. 7). Thus, this criterion is not suitable to characterise the high-impact related Vb-cyclones. Similarly, a second cross-section over France and Switzerland labelled "ATL" in Fig. 2 allows to analyse the southward moisture flux from the North Atlantic Ocean. As the right panel of Fig. 7 demonstrates, this cross-section enables a slightly clearer separation between HPEs and WPEs than the moisture fluxes across "MED" line. The increased transport of HPEs suggests that a large part of moisture is transported from the North Atlantic, instead of the Mediterranean Sea. Still, no clear separation between the HPEs and the LPEs is found, espe-

ESDD
6, 907–941, 2015

cially because it is very sensitive to the exact location of this cross-section (not shown). Hence, these results indicate that moisture variables alone do not allow to explain the different behaviour observed between HPEs and WPEs.

Once ruled out the thermodynamic state of the atmosphere as a suitable explanation of the within-Vb variability, we turn our attention to the dynamical mechanisms. Reasons for the deviations in precipitation amounts and pattern among Vb-cyclones are found more clearly in the geopotential height field. Figure 8 reveals that the WPEs overall show a smaller intensification rate than HPEs (p level < 0.01). Further differences in the geopotential height are found in the spatial structure of the average state (Fig. 9). The HPEs and WPEs show similar features at first glance in the z850 field during the most precipitation intense time step. In both cases a low pressure area is localised in the centre of the storm. This is expected as this is indeed the criterion used for the detection tool applied in the first step. Nevertheless, there are some important differences. The composites of HPEs exhibit a strong cyclone, as a steep gradient in combination with a deep depression is observed. The fact that the HPEs are triggered by a distinct cyclone is more obvious when considering higher levels, because the depression from the ground extends through the 500 and 300 hPa levels. Another indication for a strong developing cyclone is the westward tilting of the system. This is in contrast with the WPEs, which are induced by a shallow depression. Even though the z850 shows an isolated isobar, this feature is lost at the 500 hPa and appears as a weak depression at 300 hPa again. Another important feature is detected in the northwest of the WPEs in terms of a depression. This system seems to coalesce with the original depression, which leads to an asymmetric geopotential height gradient on the southern side of the cyclone centre.

The hypothesis of associating a stronger cyclone with HPEs is underlined when analysing the potential vorticity (PV) at the 325 K potential temperature surface (Fig. 10). For the HPEs, it presents a PV-streamer that is close to a cut-off. This feature is absent in the WPE cases, which show instead a PV maximum in the northwest of the cyclone centre, similar to the situation of the 300 hPa geopotential height field.

ESDD
6, 907–941, 2015

The aforementioned differences in the geopotential height fields between the HPEs and WPEs trigger important differences in the wind field in different elevations. Figure 11 shows that the wind fields at 850 hPa of the HPEs experience strong winds on the southern side of the cyclone centre, transporting air masses directly towards the northwest of the cyclone and out of its influence region. More importantly, rotation around the centre of the cyclone becomes apparent. The same features are also visible on the 325 K potential temperature surface in Fig. 10, where air masses are transported towards the northeast due to its U-shape, whereas the wind system close to the centre rotates. This rotation is highly important for high-impact Vb-cyclones (HPEs), as moisture needs to be transported around the Alps to produce orographic lifting along the northern side of the Alps. Hence, orographic precipitation is generated on the northern side of the Alps. This is supported by the fact that a major part of precipitation amounts is actually found on the northeastern side of the Alps and thus in the region of interest during the most precipitation intense time step. In contrast, WPEs do not exhibit such rotating wind field. This is mainly due to the influence of the deeper depression in the northwest of the cyclones appearing at the same time as the WPEs. The strong gradient, which is maintained at the southern side of the actual cyclone centre, results in strong U-shaped wind fields that preclude rotation. Nevertheless, a certain amount of rotation is found above the ground (not shown), which explains the modest amounts of precipitation found in the region of interest. However, the main part of the precipitation can still be detected on the southern side of the Alps, as orographic lifting occurs there. Thus, the precipitation on the southern side of the Alps is not able to influence the main precipitation area of Vb-cyclones during the most precipitation intense time step.

4 Discussion and conclusion

The results concerning the basic climatology of Vb-cyclones show a good agreement with the findings previously reported by Hofstätter and Chimani (2012), i.e., the rareness of Vb-cyclones (2.3 Vb-cyclone appearances per year, the peak of Vb-

ESDD
6, 907–941, 2015

cyclones in spring and a general agreement of the exact appearance of 65 % of all Vb-cyclones compared to Hofstätter and Chimani (2012). As our findings seem to be robust with respect to the applied method, our study goes beyond the statistical climatology introduced by Hofstätter and Chimani (2012) and deepens on the physical mechanisms in order to understand the large variability within the Vb-cyclone triggered precipitation.

The analysis of the precipitation distribution associated to Vb-cyclones reveals that the cases identified in the extended winter are not able to trigger extreme precipitation. This fact can be explained through the application of the Clausius–Claperyon equation. However, summer cases exhibit larger variability, leading to a number of extreme situations. This motivates a further subclassification. Although the moisture content in the atmosphere provides a first separation between the extended summer and winter Vb-cyclones, it fails to serve as criterion to separate the 10 WPEs and HPEs in the extended summer, since the inter case variability is too large. Also neither the northward moisture flux from the Mediterranean Sea nor the southward flux from the Atlantic can succeed in disentangling the different behaviour of WPEs and HPEs. We identify various moisture sources contributing to precipitation in Vb-events apart from the Mediterranean Sea, a result that is consistent with previous findings reported by Stohl and James (2004), James et al. (2004) and Sodemann et al. (2009) for the one-in-a-century flood in August 2002. The large amount of possible moisture source combinations and the various moisture patterns that associated to the Vb-cyclones enable us to conclude that the moisture content and source strongly depend on a case-to-case basis and preclude obtaining general conclusions.

In contrast, the variables associated to the large-scale dynamics, i.e., geopotential height and PV at the potential temperature level 325 K, allow a meaningful categorisation of the HPEs and WPEs. The average geopotential height field in HPEs shows a distinct cut-off low extending over the whole atmosphere. Additionally, PV shows a PV-streamer close to a cut-off. These two features trigger a vortex that can be traced in the wind fields. These fields suggest that precipitation is triggered by a northerly

ESDD
6, 907–941, 2015

Alpine inflow. Thus, most of the precipitation falls on the northern to north-eastern side of the Alps. Similar situations ("pivoting cut-off") have been found by Stucki et al. (2012) in the context of past extreme floods in Switzerland. Also Zängl (2004) identified the orographic enhancement as important trigger for the high precipitation records in August 2002. The WPEs in contrary are only associated with weak low pressure systems that do not elongate through various atmospheric layers. Also PV reveals only an initial state of a PV-streamer. Hence, there is no vortex visible in the wind fields. In the case of the WPEs, we conclude that the Alpine inflow takes place at the southern or south-eastern side of the Alps, which is supported by the mostly southernly located precipitation amounts. These features are similar to the "Canarian Trough" described by Stucki et al. (2012) in association with past extreme floods in Switzerland. These cyclones are strongly influenced by a low over Brittany and thus show a southwesterly flow (Stucki et al., 2012). The same is true for the WPEs, which are strongly influenced by a low in the northeast of their cyclone centres.

The fact that unlike humidity, the large-scale dynamic behaviour of the atmosphere allows a clear differentiation between the HPEs and WPEs, leads us to the conclusion that the thermodynamic state of the atmosphere only plays a secondary role in triggering heavy precipitation associated to Vb-events. These findings have important implications for a future climate change. On the one hand, an increased moisture amount is projected in the atmosphere as response to the increase in temperature with a changing climate (again associated to the Clausius–Claperyon equation). Hence, an increase in precipitation amounts can be expected in principle in the future. On the other hand, Pal et al. (2004), Yin (2005), Giorgi and Lionello (2008) and Raible et al. (2010) argue that shifts in the cyclone track, and thus changes in the more important dynamical part of a Vb-cyclone, are expected under a future climate. In particular, the former studies project a poleward shift of the storm track in a future climate, while Woollings et al. (2012) expect an eastward extension of the storm track. These projections about the changing behaviour of the storm track in the future suggests that the phenomenon Vb-cyclone could become even rarer if either of the two shifts occur. Combining these two

ESDD
6, 907–941, 2015

Climatology of Vb-cyclones, physical mechanisms

M. Messmer et al.

arguments, it can be expected that Vb-cyclones would happen more seldom, but with an increased intensity in precipitation. Nissen et al. (2013) confirmed this in a study on Vb-cyclones. However, this hypothesis is associated with a large amount of uncertainty, and a more precise assessment of the future behaviour of Vb-events and their related impacts cannot be done with the evidence exposed in this analysis. Thus, more research on the large-scale dynamic changes of different Vb-cyclone subcategories under a future climate is needed to fully understand the changes in precipitation amounts and frequency of Vb-cyclones.

Even though it is possible to find a reason for the high variability in Vb-cyclone triggered precipitation amounts, the exact triggering mechanism for precipitation cannot be found using the coarse resolution of ERA-Interim. This is especially true in the Alps where the coarse resolution is a strong limiting factor of ERA-Interim. As the Vb-cyclones are phenomena which strongly depend on mountains, more insights could be gained using regional modelling. Dynamical downscaling will not only improve the spatial resolution, but also the temporal resolution. Such higher resolved dataset will allow a closer look into thermodynamics, while an increased temporal resolution can provide additional information on dynamics (Muskulus and Jacob, 2005). Thus, future studies will consider the re-evaluation of the Vb-cyclone climatology based on high-regional downscaling products, as well as direct assessments of the evolution Vb-events through climate simulations.

Acknowledgements. The authors are grateful for the funding provided by the Dr. Alfred Bretscher-Fonds für Klima- und Luftverschmutzungsforschung. Thanks are also due to the support provided by the Oeschger Centre for Climate Change Research and the Mobiliar lab for climate risks and natural hazards (Mobilab). The ERA-Interim reanalysis data was provided by the ECMWF. Finally, we acknowledge the E-OBS dataset from the EU-FP6 project ENSEMBLES (http://ensembles-eu.metoffice.com) and the data providers in the ECA&D project (http://www.ecad.eu).

References

Bengtsson, L., Hodges, K. I., Esch, M., Keenlyside, N., Kornblueh, L., Luo, J.-J., and Yamagata, T.: How may tropical cyclones change in a warmer climate?, Tellus A, 59, 539–561, doi:10.1111/j.1600-0870.2007.00251.x, 2007. 915

Beniston, M.: August 2005 intense rainfall event in Switzerland: Not necessarily an analog for strong convective events in a greenhouse climate, Geophys. Res. Lett., 33, L05701, doi:10.1029/2005GL025573, 2006. 910

Blender, R., Fraedrich, K., and Lunkeit, F.: Identification of cyclone-track regimes in the North Atlantic, Q. J. Roy. Meteor. Soc., 123, 727–741, doi:10.1002/qj.49712353910, 1997. 913, 916, 932

Dee, D. P., Uppala, S. M., Simmons, A. J., Berrisford, P., Poli, P., Kobayashi, S., Andrae, U., Balmaseda, M. A., Balsamo, G., Bauer, P., Bechtold, P., Beljaars, A. C. M., van de Berg, L., Bidlot, J., Bormann, N., Delsol, C., Dragani, R., Fuentes, M., Geer, A. J., Haimberger, L., Healy, S. B., Hersbach, H., Hólm, E. V., Isaksen, L., Krallberg, P., Köhler, M., Matricardi, M., McNally, A. P., Monge-Sanz, B. M., Morcrette, J.-J., Park, B.-K., Peubey, C., de Rosnay, P., Tavolato, C., Thëpaut, J.-N., and Vitart, F.: The ERA-Interim reanalysis: configuration and performance of the data assimilation system, Q. J. Roy. Meteor. Soc., 137, 553–597, doi:10.1002/qj.828, 2011. 912

Donat, M. G., Pardowitz, T., Leckebusch, G. C., Ulbrich, U., and Burghoff, O.: High-resolution refinement of a storm loss model and estimation of return periods of loss-intensive storms over Germany, Nat. Hazards Earth Syst. Sci., 11, 2821–2833, doi:10.5194/nhess-11-2821-2011, 2011. 909

Fink, A. H., Pohle, S., Pinto, J. G., and Knippertz, P.: Diagnosing the influence of diabatic processes on the explosive deepening of extratropical cyclones, Geophys. Res. Lett., 39, L07803, doi:10.1029/2012GL051025, 2012. 909

Fricke, W. and Kaminski, U.: Ist die Zunahme von Starkniederschlägen auf veränderte Wetterlagen zurückzuführen, GAW Brief des Deutschen Wetterdienstes, 12, 2002. 910

Gao, X., Pal, J. S., and Giorgi, F.: Projected changes in mean and extreme precipitation over the Mediterranean region from a high resolution double nested RCM simulation, Geophys. Res. Lett., 33, L03706, doi:10.1029/2005GL024954, 2006. 911

Giorgi, F. and Lionello, P.: Climate change projections for the Mediterranean region, Global Planet. Change, 63, 90–104, doi:10.1016/j.gloplacha.2007.09.005, 2008. 924

Gómez-Navarro, J. J., Montávez, J. P., Jerez, S., Jiménez-Guerrero, P., and Zorita, E.: What is the role of the observational dataset in the evaluation and scoring of climate models?, Geophys. Res. Lett., 39, L24701, doi:10.1029/2012GL054206, 2012. 913

Grazzini, F. and van der Grijn, G.: Central European floods during summer 2002, ECMWF Newsletter, 96, 18–28, 2002. 909, 910

Haylock, M. R., Hofstra, N., Klein Tank, A. M. G., Klok, E. J., Jones, P. D., and New, M.: A European daily high-resolution gridded data set of surface temperature and precipitation for 1950–2006, J. Geophys. Res.-Atmos., 113, D20119, doi:10.1029/2008JD010201, 2008. 913

Hofstätter, M. and Chimani, B.: Van Bebber's cyclone tracks at 700 hPa in the Eastern Alps for 1961–2002 and their comparison to circulation type classifications, Meteorol. Z., 21, 459–473, doi:10.1127/0941-2948/2012/0473, 2012. 910, 911, 915, 916, 917, 922, 923

Hofstra, N., Haylock, M., New, M., and Jones, P. D.: Testing E-OBS European high-resolution gridded data set of daily precipitation and surface temperature, J. Geophys. Res.-Atmos., 114, D21101, doi:10.1029/2009JD011799, 2009. 913

IPCC-AR4: The physical science basis, in: Contribution of Working Group I to the Fourth Assessment Report of the Intergovernmental Panel on Climate Change, edited by: Solomon, S., Qin, D., Manning, M., Chen, Z., Marquis, M., Averyt, K. B., Tignor, M., and Miller, H. L., Cambridge University Press, Cambridge, UK, and New York, NY, USA, 996 pp., 2007. 911

IPCC-SREX: Managing the Risks of Extreme Events and Disasters to Advance Climate Change Adaptation. A Special Report of Working Groups I and II of the Intergovernmental Panel on Climate Change, edited by: Field, C. B., Barros, V., Stocker, T. F., Qin, D., Dokken, D. J., Ebi, K. L., Mastrandrea, M. D., Mach, K. J., Plattner, G.-K., Allen, S. K., Tignor, M., and Midgley, P. M., Cambridge University Press, Cambridge, UK, and New York, NY, USA, 2012. 908

James, P., Stohl, A., Spichtinger, N., Eckhardt, S., and Forster, C.: Climatological aspects of the extreme European rainfall of August 2002 and a trajectory method for estimating the associated evaporative source regions, Nat. Hazards Earth Syst. Sci., 4, 733–746, doi:10.5194/nhess-4-733-2004, 2004. 909, 923

Kaspar, M. and Müller, M.: Selection of historic heavy large-scale rainfall events in the Czech Republic, Nat. Hazards Earth Syst. Sci., 8, 1359–1367, doi:10.5194/nhess-8-1359-2008, 2008. 909

ESDD
6, 907–941, 2015

Köppen, W.: Die Zugstrassen der barometrischen Minima in Europa und auf dem nordatlantischen Ocean und ihr Einfluss auf Wind und Wetter bei uns, Mittheilungen der Geographischen Gesellschaft in Hamburg, 1, 76–97, 1881. 909

Kundzewicz, Z. W., Ulbrich, U., Brücher, T., Graczyk, D., Krüger, A., Leckebusch, G. C., Menzel, L., Pińskwar, I., Radziejewski, M., and Szwed, M.: Summer floods in central Europe – climate change track?, Nat. Hazards, 36, 165–189, doi:10.1007/s11069-004-4547-6, 2005. 910, 919

Lionello, P., Dalan, F., and Elvini, E.: Cyclones in the Mediterranean region: the present and the doubled CO_2 climate scenarios, Clim. Res., 22, 147–159, doi:10.3354/cr022147, 2002. 911

Mudelsee, M., Börngen, M., Tetzlaff, G., and Grünewald, U.: Extreme floods in central Europe over the past 500 years: role of cyclone pathway “Zugstrasse Vb”, J. Geophys. Res.-Atmos., 109, D23101, doi:10.1029/2004JD005034, 2004. 910

Muskulus, M. and Jacob, D.: Tracking cyclones in regional model data: the future of Mediterranean storms, Adv. Geosci., 2, 13–19, doi:10.5194/adgeo-2-13-2005, 2005. 911, 925

Neu, U., Akperov, M. G., Bellenbaum, N., Benestad, R., Blender, R., Caballero, R., Cocozza, A., Dacre, H. F., Feng, Y., Fraedrich, K., Grieger, J., Gulev, S., Hanley, J., Hewson, T., Inatsu, M., Keay, K., Kew, S. F., Kindem, I., Leckebusch, G. C., Liberato, M. L. R., Lionello, P., Mokhov, I. I., Pinto, J. G., Raible, C. C., Reale, M., Rudeva, I., Schuster, M., Simmonds, I., Sinclair, M., Sprenger, M., Tilinina, N. D., Trigo, I. F., Ulbrich, S., Ulbrich, U., Wang, X. L., and Wernli, H.: IMILAST: a community effort to intercompare extratropical cyclone detection and tracking algorithms, B. Am. Meteorol. Soc., 94, 529–547, doi:10.1175/BAMS-D-11-00154.1, 2013. 913

Nissen, K. M., Ulbrich, U., and Leckebusch, G. C.: Vb cyclones and associated rainfall extremes over Central Europe under present day and climate change conditions, Meteorol. Z., 22, 649–660, doi:10.1127/0941-2948/2013/0514, 2013. 910, 911, 925

Nissen, K. M., Leckebusch, G. C., Pinto, J. G., and Ulbrich, U.: Mediterranean cyclones and windstorms in a changing climate, Reg. Environ. Change, 14, 1873–1890, doi:10.1007/s10113-012-0400-8, 2014. 911

Pal, J. S., Giorgi, F., and Bi, X.: Consistency of recent European summer precipitation trends and extremes with future regional climate projections, Geophys. Res. Lett., 31, L13202, doi:10.1029/2004GL019836, 2004. 924

Pinto, J. G., Spangehl, T., Ulbrich, U., and Speth, P.: Assessment of winter cyclone activity in a transient ECHAM4-OPYC3 GHG experiment, Meteorol. Z., 15, 279–291, doi:10.1127/0941-2948/2006/0128, 2006. 911

Raible, C. C.: On the relation between extremes of midlatitude cyclones and the atmospheric circulation using ERA40, Geophys. Res. Lett., 34, L07703, doi:10.1029/2006GL029084, 2007. 909

Raible, C. C., Della-Marta, P. M., Schwierz, C., Wernli, H., and Blender, R.: Northern Hemisphere extratropical cyclones: a comparison of detection and tracking methods and different reanalyses, Mon. Weather Rev., 136, 880–897, doi:10.1175/2007MWR2143.1, 2008. 913

Raible, C. C., Ziv, B., Saaroni, H., and Wild, M.: Winter synoptic-scale variability over the Mediterranean Basin under future climate conditions as simulated by the ECHAM5, Clim. Dynam., 35, 473–488, doi:10.1007/s00382-009-0678-5, 2010. 911, 924

Sodemann, H., Wernli, H., and Schwierz, C.: Sources of water vapour contributing to the Elbe flood in August 2002 – a tagging study in a mesoscale model, Q. J. Roy. Meteor. Soc., 135, 205–223, doi:10.1002/qj.374, 2009. 909, 920, 923

Stohl, A. and James, P.: A Lagrangian analysis of the atmospheric branch of the global water cycle. Part I: Method description, validation, and demonstration for the August 2002 flooding in Central Europe, J. Hydrometeorol., 5, 656–678, doi:10.1175/1525-7541(2004)005<0656:ALAOTA>2.0.CO;2, 2004. 909, 920, 923

Stucki, P., Rickli, R., Brönnimann, S., Martius, O., Wanner, H., Grebner, D., and Luterbacher, J.: Weather patterns and hydro-climatological precursors of extreme floods in Switzerland since 1868, Meteorol. Z., 21, 531–550, doi:10.1127/0941-2948/2012/368, 2012. 924

Stucki, P., Brönnimann, S., Martius, O., Welker, C., Imhof, M., von Wattenwyl, N., and Philipp, N.: A catalog of high-impact windstorms in Switzerland since 1859, Nat. Hazards Earth Syst. Sci., 14, 2867–2882, doi:10.5194/nhess-14-2867-2014, 2014. 909

Trigo, I. F., Davies, T. D., and Bigg, G. R.: Objective climatology of cyclones in the Mediterranean region, J. Climate, 12, 1685–1696, doi:10.1175/1520-0442(1999)012<1685:OCOCIT>2.0.CO;2, 1999. 910

Ulbrich, U., Brücher, T., Fink, A. H., Leckebusch, G. C., Krüger, A., and Pinto, J. G.: The central European floods of August 2002: Part 1 – Rainfall periods and flood development, Weather, 58, 371–377, doi:10.1256/wea.61.03A, 2003a. 909, 919

ESDD
6, 907–941, 2015

Ulbrich, U., Brücher, T., Fink, A. H., Leckebusch, G. C., Krüger, A., and Pinto, J. G.: The central European floods of August 2002: Part 2 – Synoptic causes and considerations with respect to climatic change, Weather, 58, 434–442, doi:10.1256/wea.61.03B, 2003b. 909

Van Bebber, W.: Die Zugstrassen der barometrischen Minima nach den Bahnenkarten der deutschen Seewarte für den Zeitraum 1875–1890, Meteorol. Z. [Offprint], 8, 361–366, 1891. 909, 917

Woollings, T., Gregory, J. M., Pinto, J. G., Reyers, M., and Brayshaw, D. J.: Response of the North Atlantic storm track to climate change shaped by ocean-atmosphere coupling, Nat. Geosci., 5, 313–317, doi:10.1038/ngeo1438, 2012. 924

Yin, J. H.: A consistent poleward shift of the storm tracks in simulations of 21st century climate, Geophys. Res. Lett., 32, L18701, doi:10.1029/2005GL023684, 2005. 924

Zängl, G.: Numerical simulations of the 12–13 August 2002 flooding event in eastern Germany, Q. J. Roy. Meteor. Soc., 130, 1921–1940, doi:10.1256/qj.03.152, 2004. 924

ESDD
6, 907–941, 2015
Climatology of Vb-cyclones, physical mechanisms
M. Messmer et al.

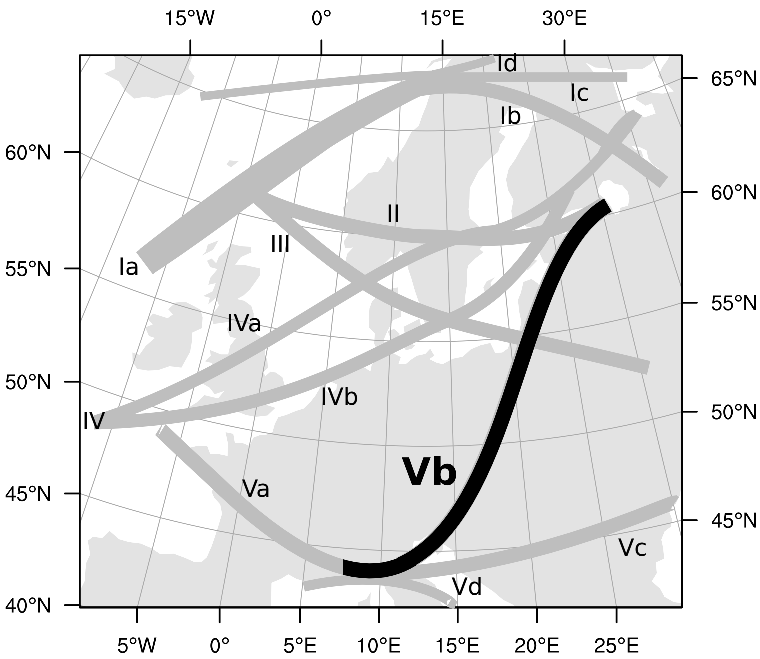

Figure 1. Trajectories of the barometric minima between 1876–1880, as defined by W. J. van Bebber in 1981. The trajectory that defines Vb-cyclones is highlighted in black.

ESDD
6, 907–941, 2015

Climatology of Vb-cyclones, physical mechanisms

M. Messmer et al.

ESDD
6, 907–941, 2015

Climatology of Vb-cyclones, physical mechanisms

M. Messmer et al.

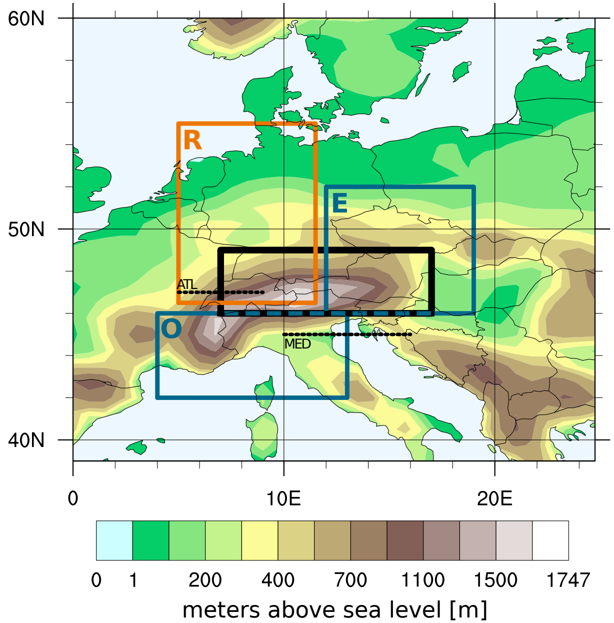

Figure 2. The three boxes used to automatically filter out the Vb-cyclones from the total number of cyclones found by the tracking technique (Blender et al., 1997). O, E and R denote the origin, the end and the restriction box, respectively. The black box over the alpine region defines the area of interest for precipitation amounts. The two stippled black lines indicate the position of the two cross-sections used to calculate the moisture flux. The topography corresponds to the one implemented in ERA-Interim.

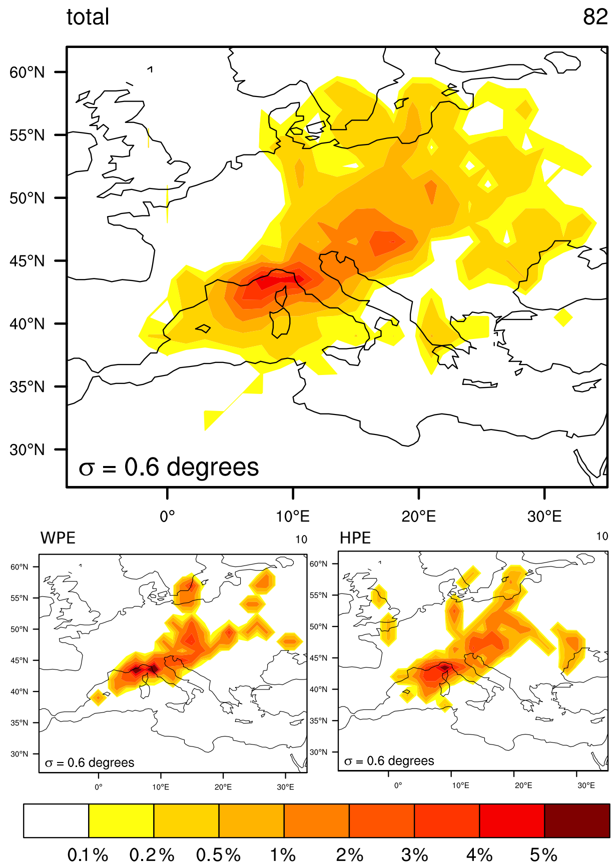

Figure 3. Probability density field of all detected Vb-cyclone centers (top panel), of the heavy precipitation events (HPEs) (bottom left panel) and of the weak precipitation events (WPEs) (bottom right panel). The shading shows how probable it is that a Vb-cyclone centre is located at the according grid point at any time step in the 1979–2013 period.

ESDD
6, 907–941, 2015

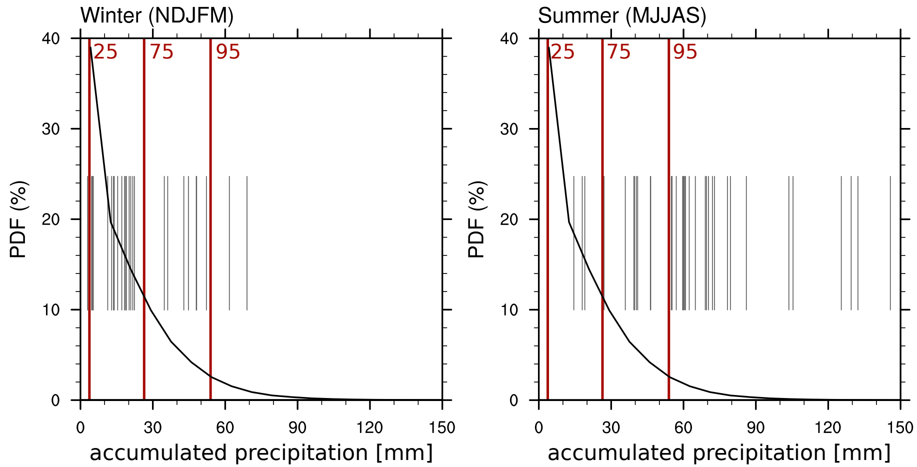

Figure 4. Probability density function of the accumulated precipitation from ERA-Interim of Vb-events (black line) for extended winter (left panel) and extended summer (right panel). The red lines indicate the 25, 75 and 95 percentile from left to right. The vertical, black lines indicate the accumulated precipitation of all Vb-cyclones occurring during each season, respectively.

ESDD
6, 907–941, 2015

M. Messmer et al.

Title Page
Abstract | Introduction
Conclusions | References
Tables | Figures
◂ | ▸
Back | Close
Full Screen / Esc
Printer-friendly Version
Interactive Discussion

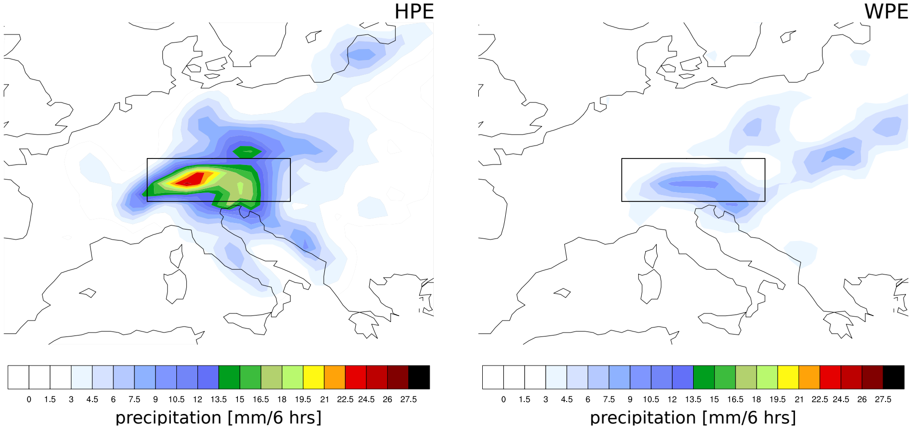

Figure 5. Average precipitation during the time step with maximum precipitation for the 10 HPEs (left panel) and the 10 WPEs (right panel). The black box indicates the precipitation region of interest, depicted also in Fig. 2 as black rectangle.

ESDD
6, 907–941, 2015

Climatology of Vb-cyclones, physical mechanisms

M. Messmer et al.

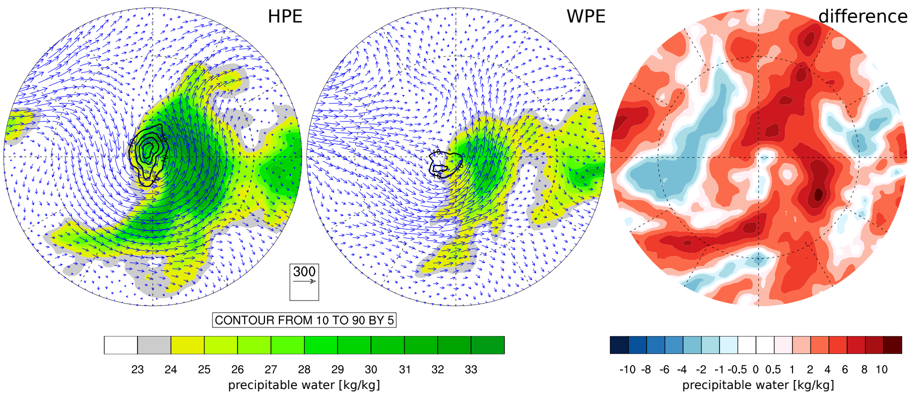

Figure 6. Composites of precipitable water content [$\mathrm{kg\,kg^{-1}}$, shading] and precipitation amounts (black contours) for the HPEs (left panel) and for the WPEs (centre panel). Additionally the moisture flux is shown by arrows integrated over the vertical structure of the atmosphere (reference vector: 300 $\mathrm{kg\,m\,kg^{-1}\,s^{-1}}$). The time step with maximum precipitation is shown for all variables. The differences in precipitable water between HPEs and WPEs is shown (right panel).

ESDD
6, 907–941, 2015
Climatology of Vb-cyclones, physical mechanisms
M. Messmer et al.

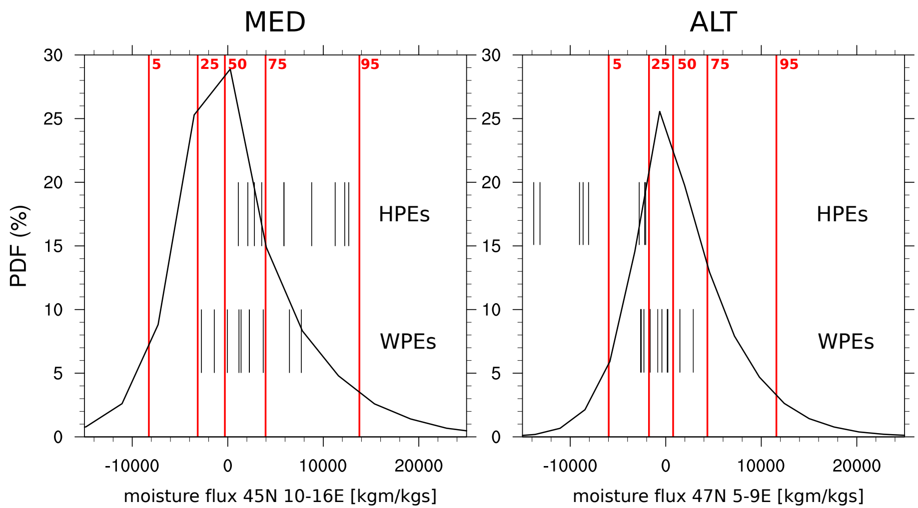

Figure 7. Probability density function of the accumulated moisture flux of all Vb-events (black line). The vertical top (bottom) lines indicate the accumulated moisture flux of the HPEs (WPEs) through the stippled black lines depicted in Fig. 2 labelled with "MED" (left panel) and labelled with "ATL" (right panel). The red lines indicate the 5, 25, 50, 75 and 95 percentile from left to right.

ESDD
6, 907–941, 2015

Climatology of Vb-cyclones, physical mechanisms

M. Messmer et al.

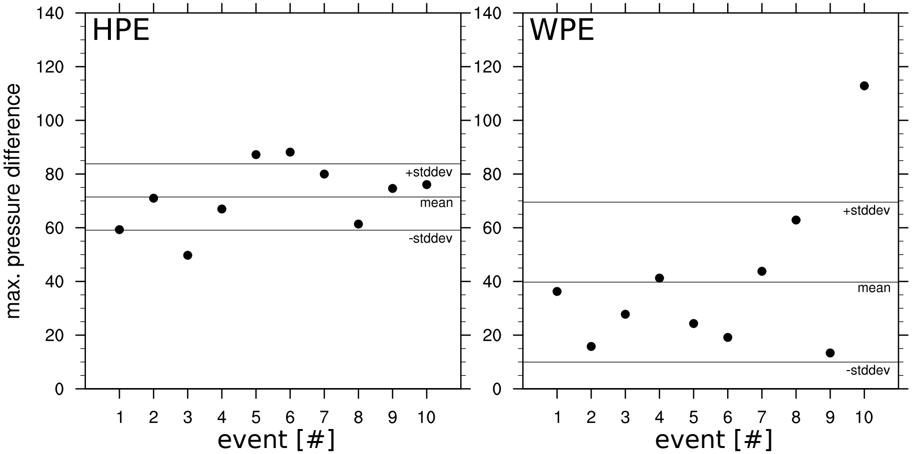

Figure 8. Difference between the minimum and maximum pressure during the entire life cycle for the HPEs (left panel) and WPEs (right panel). The events are sorted according to precipitation produced in the target area (Fig. 2), with #1 being the most extreme precipitation event. The three horizontal black lines indicate the mean and the standard deviation, respectively.

ESDD
6, 907–941, 2015
Climatology of Vb-cyclones, physical mechanisms
M. Messmer et al.

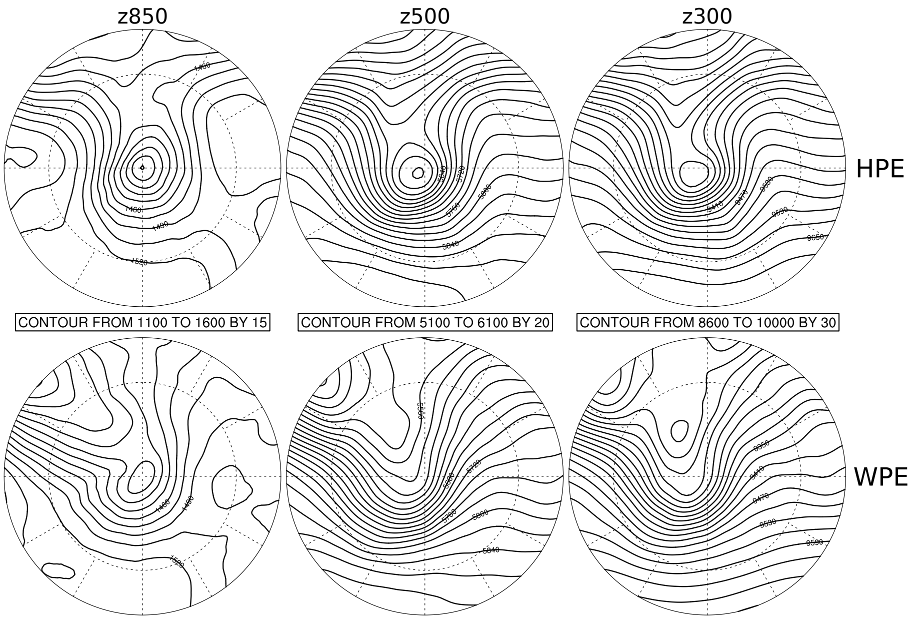

Figure 9. Average geopotential height at 850 hPa (left column), 500 hPa (centre column) and 300 hPa (right column) for the time step with maximum precipitation of all HPEs (upper row) and WPEs (bottom row).

ESDD
6, 907–941, 2015

Climatology of Vb-cyclones, physical mechanisms

M. Messmer et al.

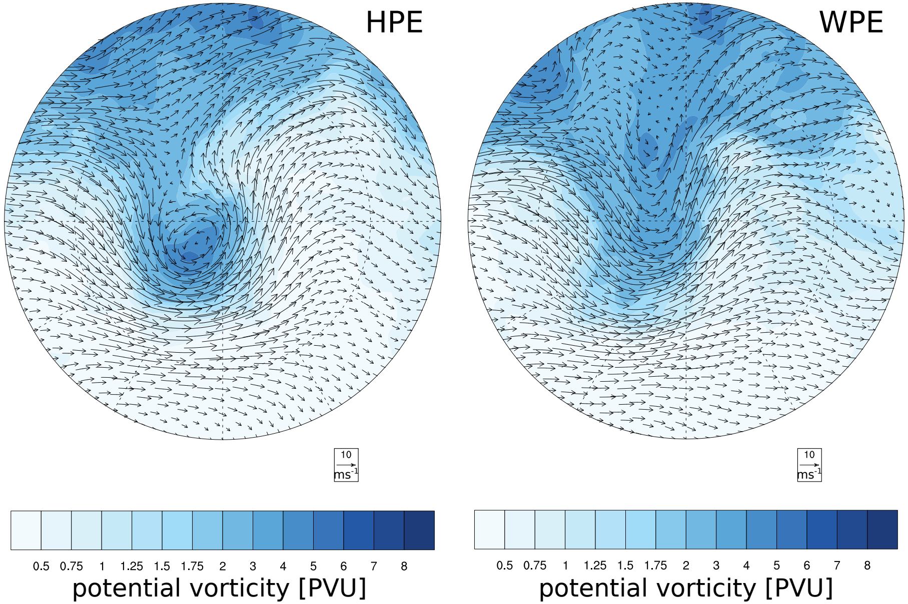

Figure 10. Composites of potential vorticity [PVU, shading] on the 325 K potential temperature surface at the time step with maximum precipitation of the HPEs (left panel) and the WPEs (right panel). Wind fields are also shown for the 325 K potential temperature surface (reference vector: 10 m s^{-1}).

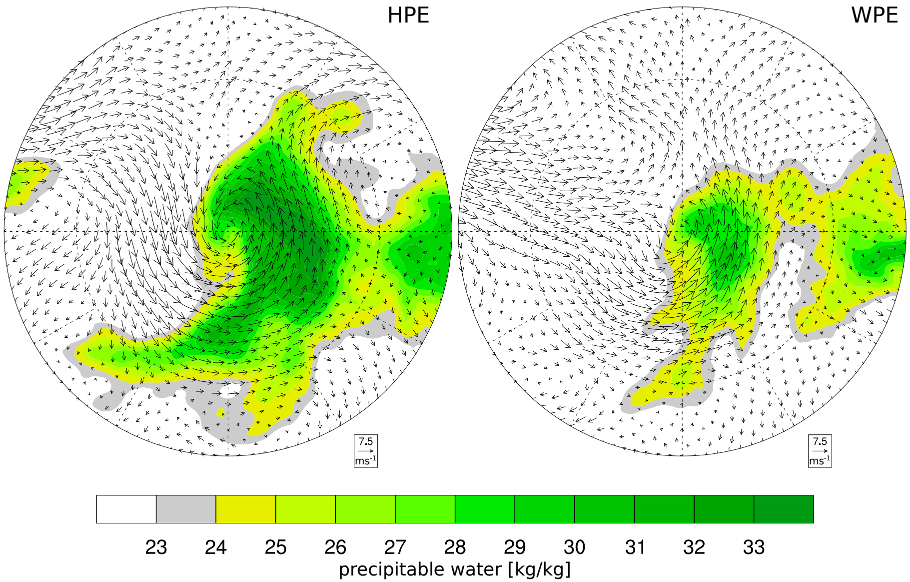

Figure 11. Composites of precipitable water content [kg kg^{-1}, shading] and wind fields at 850 hPa (reference vector 7.5 m s^{-1}) during the time step of maximum precipitation for the HPEs (left panel) and the WPEs (right panel).

ESDD
6, 907–941, 2015

Climatology of Vb-cyclones, physical mechanisms

M. Messmer et al.